Hindawi Publishing Corporation
X-Ray Optics and Instrumentation
Volume 2010, Article ID 743485, 17 pages
doi:10.1155/2010/743485

Review Article

Diffractive X-Ray Telescopes

Gerald K. Skinner[1,2]

[1] *CRESST and NASA-GSFC, Greenbelt, MD 20771, USA*
[2] *Department of Astronomy, University of Maryland, College Park, MD 20742, USA*

Correspondence should be addressed to Gerald K. Skinner, skinner@milkyway.gsfc.nasa.gov

Received 25 February 2010; Accepted 17 August 2010

Academic Editor: Stephen L. O'Dell

Diffractive X-ray telescopes using zone plates, phase Fresnel lenses, or related optical elements have the potential to provide astronomers with true imaging capability with resolution several orders of magnitude better than available in any other waveband. Lenses that would be relatively easy to fabricate could have an angular resolution of the order of microarcseconds or even better, that would allow, for example, imaging of the distorted spacetime in the immediate vicinity of the supermassive black holes in the center of active galaxies What then is precluding their immediate adoption? Extremely long focal lengths, very limited bandwidth, and difficulty stabilizing the image are the main problems. The history and status of the development of such lenses is reviewed here and the prospects for managing the challenges that they present are discussed.

1. Introduction

Diffractive optics, in the form of zone plates and various forms of Fresnel lenses and kineforms, already play a major role in the manipulation of X-ray beams at synchrotron facilities and in X-ray microscopy. Diffractive X-ray telescopes, in contrast, exist almost entirely as concepts on paper and as proposals and suggestions, though as will be seen demonstrations of scaled systems have been made. Because of atmospheric absorption, their potential application is almost certainly limited to astronomy (and specifically to astronomy from space), perhaps including solar and planetary studies. However, for certain objectives within that field they present the prospect of enormous advances over current instrumentation, which relies largely on grazing incidence reflective optics (reviewed elsewhere in this series [1–3]). The most notable prospect that diffractive telescopes offer is that of superb angular resolution, with improvements of perhaps six orders of magnitude on the current state of the art. But even neglecting benefits from the imaging properties, their capability of concentrating the flux received over a large effective area onto a small, and hence low background, detector may also offer unique advantages in some circumstances.

This paper will consider the various concepts that have been proposed and discuss the current state of development of the technologies necessary to turn the ideas into a real system. For simplicity the term X-rays will often be used to apply to both X-rays and gamma rays, there being no clear distinction or borderline between the two. The paper will be limited to techniques exploiting the wave nature of X-ray (and gamma ray) radiation, so excluding, for example, the use of screens with zone-plate-like patterns singly as coded masks [4] or in pairs to produce Moiré fringes [5, 6]. Within wave optics, systems based on multilayer optics or on crystal diffraction are not addressed (the latter are reviewed elsewhere in this series [7]).

2. History

The basic diffractive optics imaging element can be considered to be the zone plate (ZP) in which an aperture is divided into transparent and opaque regions according to whether radiation passing through them would arrive at some selected focal point with a phase such as to interfere constructively or destructively. The resulting pattern is shown in Figure 1(a). The first zone plate was made by Lord Rayleigh in 1871 though this work was never published (see [8, 9]) and it was Soret [10] who first described them in print in 1875. Already in 1888 Rayleigh [11] realized that problems of high background due to undiffracted light and

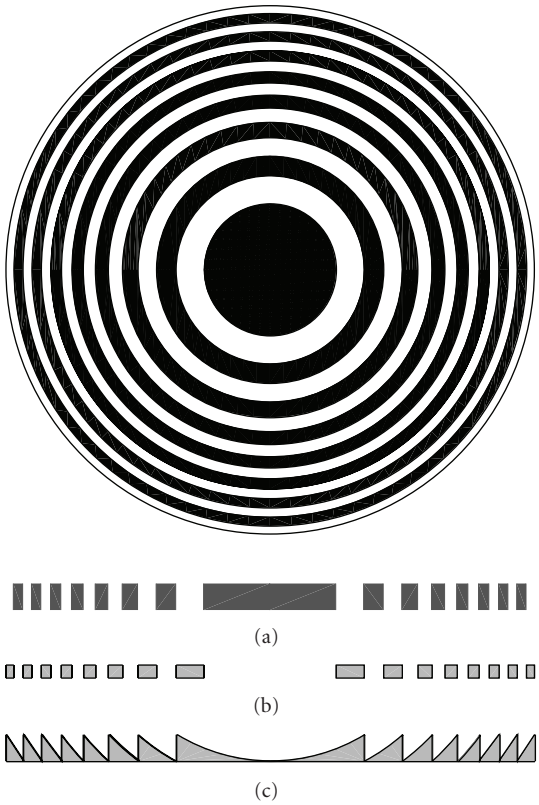

Figure 1: Three basic forms of diffractive optics for X-ray telescopes. (a) A zone plate (ZP), with opaque and transparent regions, (b) A phase zone plate (PZP), in which the shaded zones transmit radiation with a phase shift of π, (c) A phase Fresnel lens (PFL), in which the thickness is everywhere such that the phase is shifted by the optimum angle. The profile in (c) is drawn for a converging lens assuming the refractive index is less than unity.

low efficiency could be overcome by using phase-reversal zone plates (PZPs) in which the opaque regions are replaced by ones whose thickness is chosen to introduce a phase shift of π (Figure 1(b)). Wood demonstrated the operation of PZPs ten years later [12]. Miyamoto [13] further extended the concept, introducing the term phase Fresnel lens (PFL below) for an optic in which the phase shift is at each radius the same as that for an ideal conventional lens (Figure 1(c)).

The possibility of using ZPs for X-ray imaging seems first to have been seriously considered in the 1950s by Myers [14] and by Baez [15], who were concerned with X-ray microscopy. In 1974 Kirz [9] pointed out that the relative transparency of materials in the X-ray band and the fact that X-ray refractive indices differ slightly from unity would allow PZPs to be constructed even for high energy photons, so obtaining much higher efficiency.

Remarkably, as early as the 1960s simple zone plates were used for solar (soft) X-ray astronomy. Elwert [16] obtained the agreement of Friedmann to replace the pinholes in two of the pinhole cameras on a 1966 NRL solar-viewing sounding rocket flight with small zone plates designed to operate in lines at 51 Å (0.246 keV) and 34 Å (0.367 keV). Although the attitude control malfunctioned, blurred images were obtained. Over the next few years the technique was used, in particular by the Tübingen and Utrecht groups, for solar imagery from sounding rockets at energies up to 0.8 keV (e.g., [17, 18]). One of the disadvantages of zone plates proved to be the halo due to zero-order diffraction surrounding the focal point of a simple zone plate. Ways were found of alleviating this problem by using only the zones within an annular region [19, 20].

At much the same time Wolter I grazing incidence telescopes were becoming available for soft X-ray solar imaging—the first was flown on a sounding rocket in 1965 [21] and two were used on the Apollo Telescope mount on Skylab [22]. With the size of instrumentation that was feasible at that epoch, the grazing incidence technology proved superior. For cosmic observations as well as solar, it has become the imaging technique of choice except where the need for very wide fields of view or operation at high energies precludes its use, in which case nonfocussing devices such as coded mask or Compton telescopes are used.

As a result of the success of grazing angle reflective optics, diffractive X-ray optics for astronomical applications tended to be forgotten. In a 1974 PhD thesis Niemann [23] did discuss the possible use of diffractive optics for extra-solar astronomy and in 1996 Dewey et al. [24] proposed a mission concept in which patched blazed diffraction gratings based on the technology developed for the AXAF mission (now Chandra) would approximate a PZP. But it is only comparatively recently that there has been a revival of interest in the possibility of using diffractive optics for X-ray and gamma-ray astronomy in particular circumstances where it may offer unique advantages. Several authors (e.g., [25–30]) have pointed out that the angular resolution potentially available with diffractive X-ray telescopes exceeds by many orders of magnitude the practical limits of reflective optics.

Meanwhile there have been major advances in diffractive X-ray optics for nonastronomical applications, driven in particular by the availability of synchrotron sources and interest in X-ray microscopy with the best possible spatial resolution. For reasons discussed below, most of the effort has been towards lenses with structures on an extremely small scale, even if the diameter is also small. For astronomical telescopes on the other hand fineness of structure would be of secondary importance, but large apertures are essential.

3. Theory

3.1. Basic Parameters. A zone plate such as illustrated in Figure 1(a) can be conveniently characterized by the outside diameter, d, and the pitch, $p_{\min}$ of one cycle of the opaque/transparent pattern at the periphery where it is smallest (the number of cycles is assumed to be large so that a local characteristic period can be defined). The focal length for radiation of wavelength λ is then given by

$$f = \frac{p_{\min} d}{2\lambda}, \tag{1}$$

a relationship that applies equally to PZPs and PFLs. In terms of photon energy E and physical units this becomes

$$f = 403.3\left(\frac{p_{\min}}{1\,\mu\text{m}}\right)\left(\frac{d}{1\,\text{m}}\right)\left(\frac{E}{1\,\text{keV}}\right)\text{m}, \tag{2}$$

making clear that focal lengths of systems of interest for X-ray astronomy are likely to be long.

Diffractive X-ray optics has so far been employed almost exclusively for microscopy and for other applications for which *spatial* resolution is all important, but for telescopes, it is the *angular* resolution that counts. For ideal PFLs one can use the usual rule that the diffraction-limited angular resolution expressed as half-power diameter (HPD) is

$$\begin{aligned}\Delta\theta_d &= 1.03\,\frac{\lambda}{d} \\ &= 263\left(\frac{E}{1\,\text{keV}}\right)^{-1}\left(\frac{d}{1\,\text{m}}\right)^{-1}\ \text{micro-arcseconds}\ (\mu'') \qquad (3)\\ &= 0.501\left(\frac{p_{\min}}{f}\right), \qquad (4)\end{aligned}$$

(using the Rayleigh criterin, the numerical factor 1.03 would be the familiar 1.22). The same expression can in practice be used for ZPs and PZPs with a large number of cycles (Stigliani et al. [31] present an exact solution). Assuming a simple single lens system, the corresponding dimension in the image plane is then

$$\Delta x = f\Delta\theta_d = 0.501\,p_{\min}. \tag{5}$$

This is also approximately the spatial resolution of a microscope with a diffractive lens, explaining why the main drive in X-ray diffractive optics technology has so far been towards reducing $p_{\min}$. ZPs with zones of less than 15 nm, corresponding to $p_{\min} < 30$ nm, have been reported [32]. If the angular resolution of a telescope is to be limited only by diffraction, then it is important that the distance Δx be larger than the spatial resolution of the detector. Equation (5) then implies that $p_{\min}$ should *not* be too small. Current state of the art detectors have pixel sizes from 5–10 μm (CCDs at X-ray energies) to a fraction of a millimeter (pixelized CZT or Ge detectors for hard X-rays and gamma-rays). Although the centroid of the released charge can in some circumstances be localized to better than one pixel, the range of the electron which receives energy from the incoming photon sets a limit on the spatial resolution that can be obtained. So $p_{\min}$ for diffraction-limited X-ray telescopes is likely to be at least of the order of tens to hundreds of microns.

3.2. Lens Profile. A simple zone plate is inefficient because it is only 50% transmitting and because much of the radiation is not diffracted into the primary focus (order $n = 1$) but is undiffracted ($n = 0$) or diffracted into secondary focii ($n < 0$, $n > 1$). Table 1 shows that even if it is perfect the efficiency of a ZP is only ~10%.

For a ZP the depth of the profile is simply dictated by the requirement that the material be adequately opaque; the only upper limit is that imposed by manufacturing considerations. High density, high atomic number, materials are generally to be preferred. Taking Tungsten as an example and assuming 45% open area to provide for support structures, 90% opacity implies 130 gm^{-2} at 10 keV or 2.9 kg m^{-2} at 100 keV.

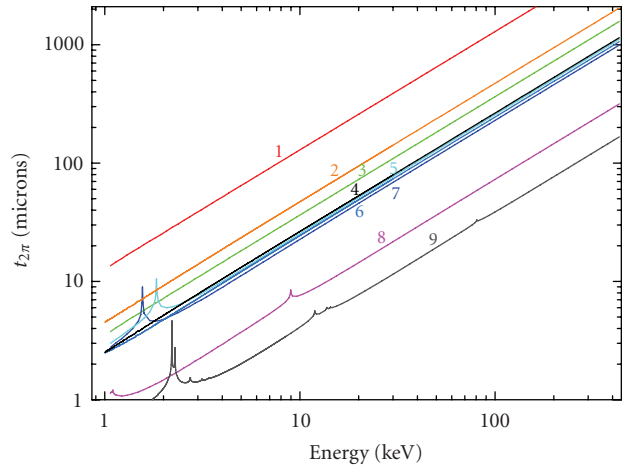

FIGURE 2: The thickness, $t_{2\pi}$, necessary to shift the phase of X-rays by 2π for some example materials. From top to bottom Li (1, red) Li, Polycarbonate (2, orange), Be (3, green), B_4C (4, light blue), Si (5, cyan), LiF (6, light blue), Al (7, dark blue), Cu (8, violet), and Au (9, grey).

For PZPs and PFLs on the other hand, the thickness of the profile and the transparency of the material are critical. The nominal thickness of a PZP is that which produces a phase shift of π. The complex refractive index of the material may be written

$$\mu = 1 - \frac{r_e\lambda^2}{2\pi}n_0(f_1 + if_2) = 1 - \delta - i\beta, \tag{6}$$

where r_e is the classical electron radius, n_0 is the number of atoms per unit volume, and $f = f_1 + if_2$ is the atomic scattering factor. The required thickness is then $(1/2)t_{2\pi}$, where $t_{2\pi}$ is λ/δ. Well above the energy of any absorption edges f_1 approaches the atomic number, so δ is proportional to λ^2 and $t_{2\pi}$ to λ^{-1}, or to E.

The practicability of X-ray PZPs relies on the fact that although the wavelengths λ are extremely short, δ is also very small. Consequently $t_{2\pi}$ is in a range, from microns to millimeters, where fabrication is practicable and where the absorption losses in traversing the required thickness of material are not too serious. Figure 2 shows some values of $t_{2\pi}$ as a function of photon energy for some materials of interest.

In the case of PFLs, the surface of each ring is ideally part of a paraboloid. This is evident if the lens is regarded as a thick refractive lens with the thickness reduced by multiples of $t_{2\pi}$. Usually the maximum height is $t_{2\pi}$ though $t_{4\pi}t_{6\pi}\cdots$ lenses can be made, with a correspondingly reduced number of rings. At large radii the small sections of paraboloids are almost straight and the cross-section is close to a triangular sawtooth. With some fabrication techniques it is convenient

Table 1: Comparison of the efficiency of ideal zone plates (ZPs), phase zone plates (PZPs), and phase Fresnel lenses (PFLs).

	Efficiency (primary focus) $n = 1$	Lost to absorption	Undiffracted $n = 0$	Secondary foci $n = -1, \pm 3, \pm 5 \cdots$
ZP	$1/\pi^2 = 10.1\%$	50%	25%	14.9%
PZP	$4/\pi^2 = 40.5\%$	0	0	59.5%
PFL	100%	0	0	0

Table 2: The primary focus efficiency, in the absence of absorption, of a stepped approximation to a PFL (see [34]).

Levels	2 (PZP)	3	4	8	16	n
Efficiency	40.5%	68.4%	81.1%	95.0%	98.7%	$\mathrm{sinc}^2(\pi/n)$

to use a stepped approximation to the ideal profile (e.g., [33]). High efficiency can be obtained with a relatively small number of levels (Table 2). Fabrication "errors" in the form of rounding of corners will actually tend to *improve* efficiency.

In contrast to ZPs, because of their lower absorption (see Section 3.5) low atomic numbers materials will generally be preferred for the fabrication of PZPs and PFLs. The low density that tends to be associated with low atomic number can however be something of a disadvantage as it implies larger $t_{2\pi}$ and so higher aspect ratio for the profile. In fact for a given photon energy the areal density of the active part of such devices is relatively independent of the material chosen. Typical values are only 30 gm^{-2} at 10 keV or 300 gm^{-2} at 100 keV. The additional mass of a substrate and/or support structure must be taken into account, but diffractive X-ray optics are intrinsically *very* light weight.

3.3. Field of View. Young [35] has discussed the off-axis aberrations of ZPs and the same conclusions can be applied to PZPs and in practice to PFLs. The expressions that he derives imply that in circumstances of interest for astronomy the most important Seidel aberration is coma, which only becomes important at off-axis angles greater than $4\lambda f^2/d^3$. In other terms, this implies that the number of diffraction-limited resolution elements across the coma-free field of view is $\sim 8(f/d)^2$. With the very large focal ratios that seem to be inevitable for diffractive X-ray telescopes, aberrations are entirely negligible over a field of view far larger than any practicable detector.

3.4. Chromatic Aberration and Other Limits to Angular Resolution. As well as the limit imposed by diffraction, given in (4), two other considerations are important for the angular resolution. The most important is the limit imposed by chromatic aberration. It is apparent from (2) that the focal length of a diffractive lens varies in proportional to the photon energy. At an energy E' away from the nominal energy E, radiation will converge in a cone towards a displaced focus (Figure 4). In the absence of diffraction, purely geometric considerations imply that this would lead to a focal spot corresponding to an angular size

$$\left|\frac{E' - E}{E}\right|\left(\frac{d}{f}\right). \tag{7}$$

Unless the spectrum of the radiation being imaged is a very narrow line with negligible continuum emission, blurring due to photons with energy other than the nominal energy has to be taken into account. Fortunately modern X-ray detectors of interest for the low flux levels that are encountered in astronomy are photon counting and energy resolving. Thus photons of energy outside a defined bandwidth can be disregarded when analyzing the data. Consequently in the most common case of a broad line and/or continuum spectrum it is the energy resolution of the detector that has to be used for ΔE in (7) and that dictates the degree of chromatic aberration.

At X-ray energies the most widely used imaging detectors are CCDs, that typically have an energy resolution of $\sim$150 eV at 6 keV, corresponding to $\Delta E/E = 2.5\%$, or active pixel sensors with similar capability [36]. In the 100–1000 keV region Germanium detectors can achieve $\Delta E/E \sim 0.25\%$–1%, though the (fractional) resolution is not as good at lower energies. Position-sensitive Germanium detectors are now becoming available (see e.g., [37], where the possibility of their use in a "Compton" configuration to reduce background by selecting only those events that are consistent with photons that may have passed through a lens is also discussed). Pixelated CZT arrays are approaching the performance of Germanium detectors and do not need cooling (Li et al. [38] report 0.61%–1.64% at 662 keV for a variety of single pixel detectors and small arrays). Microcalorimeter detectors are reaching energy resolutions of 2.5–5 eV at 6 keV [39, 40], corresponding to $\Delta E/E \sim 0.05\%$, but this performance is currently only achieved in single detector elements or small arrays. Braig and Predehl [30] have even suggested that a Bragg crystal monochromator might be used in the focal plane of a diffractive telescope and that $\Delta E/E \sim 0.01\%$ might be achieved in this way.

As discussed in Section 3.1, the spatial resolution of the detector can be important as well. The net resolution is thus in general a combination of three components

Diffraction. Rewriting the expression in (4) in terms of energy for consistency

$$\Delta\theta_d = \frac{1.03}{d}\frac{hc}{E}. \tag{8}$$

Chromatic Aberration. Equation (7) allows the *maximum* extent of the spread due to chromatic aberration, and in the absence of effects due to diffraction, to be written

$$\Delta\hat{\theta}_c = \frac{1}{2}\frac{d}{f}\frac{\Delta E}{E}. \tag{9}$$

Detector Resolution. Characterizing this by a pixel size, one has

$$\Delta\theta_p = \frac{\Delta x}{f}. \tag{10}$$

Diffraction limited performance will only be obtainable if the second and third components are negligible compared to the first. The energy bandwidth could be estimated by comparing $\Delta\theta_d$ and $\Delta\hat{\theta}_c$, but as these are different measures of the widths of very different PSF profiles a better approach is to consider the range of energies for which the wavefront error at the edge of the lens remains below some value. It is usual to place the comparatively strict limit of $\lambda/4$ corresponding to a Strehl ratio (the ratio between the peak brightness and that for an ideal, diffraction-limited system) of $8/\pi^2 \sim 80\%$. Yang [41] use a limit twice as large and other criteria lead to even wider bandwidths. For $\lambda/4$ it is found [35] that

$$\frac{\Delta E}{E} = 4\frac{f}{d^2}\frac{hc}{E} = \frac{1}{N_F}, \tag{11}$$

where N_F is the number of Fresnel zone in the PFL (twice the number of periods for a $t_{2\pi}$ lens).

3.5. Absorption. The efficiencies discussed so far ignore absorption. In evaluating such effects a key parameter is the critical Fresnel number defined by Yang [41]

$$N_0 = \frac{\delta}{2\pi\beta} = \frac{2}{t_{2\pi}\mu_{\text{abs}}}, \tag{12}$$

where $\mu_{\text{abs}} = 4\pi\beta/\lambda$ is the linear absorption coefficient. N_0 measures the relative importance of refraction and absorption. It can be thought of as the number of Fresnel zones in a refractive lens whose maximum thickness is equal to the absorption length. Example values are shown in Figure 3.

Kirz [9] has shown how in the presence of significant absorption the optimum thickness of a PZP is somewhat lower than $t_{2\pi}/2$. For $\beta/\delta = 1$ the (primary focus) efficiency is maximized if the thickness is reduced to 0.73 of this value. Similarly it can be shown that the efficiency of a PFL made from a material in which the absorption is important is maximized if the profile is modified as shown in Figure 5. Nöhammer et al. [42] discuss this issue in more detail. Efficiencies with and without this adjustment are shown as a function of N_0 in Figure 6. The improvement is not large, but the modified profile is actually likely to be lighter and easier to fabricate. Note that the optimum form would be different if the objective were to minimize either the undiffracted (zero-order) flux or that in higher orders, rather than maximize the flux diffracted into the prime focus.

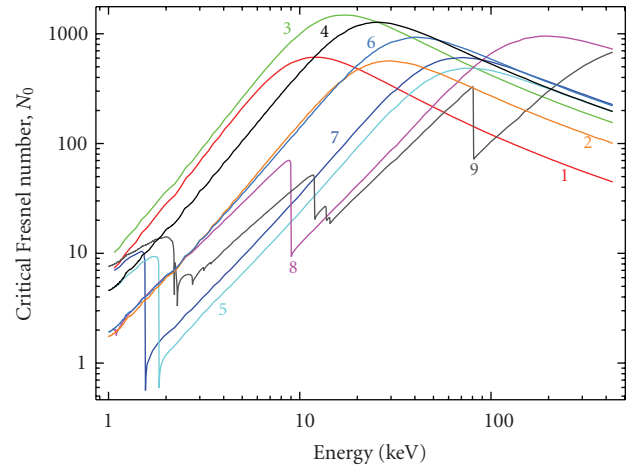

Figure 3: The critical Fresnel number, N_0, for some example materials. Numbers, colors, and materials as in Figure 2.

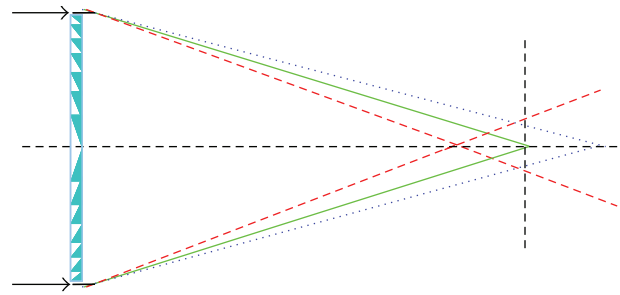

Figure 4: The effect of chromatic aberration. As the focal length of a diffractive lens is proportional to photon energy, ignoring diffraction, at energies differing by δE from the nominal energy E radiation converges in a cone and intercepts the detector plane in a disc of size given by (7).

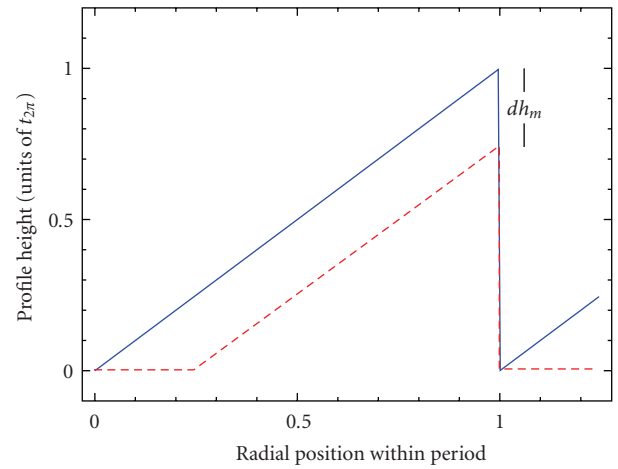

Figure 5: If significant absorption is taken into account the efficiency of a PFL can be improved by modifying the profile because improved throughput can be obtained at the expense of some phase error. The shape of the profile of a PFL that gives maximum efficiency for diffraction into the primary focus is shown by the dashed line.

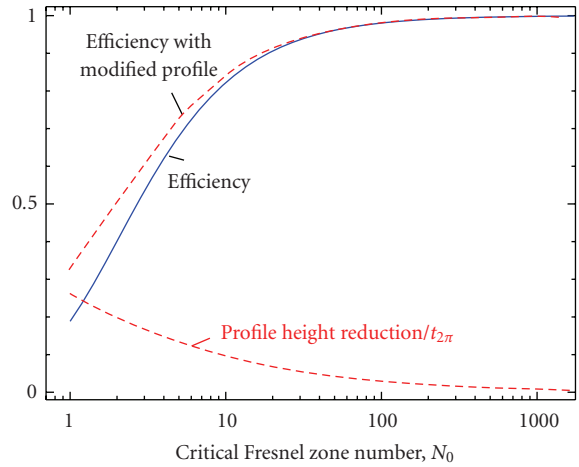

FIGURE 6: The efficiency of a PFL with significant absorption as a function of the critical fresnel number, N_0, of the material from which it is made. Also shown are the fractional amount, dh_m, by which the nominal profile height of $t_{2\pi}$ should be reduced as in Figure 5 to optimize the performance and the resulting efficiency.

4. The Advantages and Potential

4.1. Fabrication and Tolerances. Compared with grazing incidence optics of a comparable aperture, diffractive optics for X-ray astronomy are expected to be relatively simple to fabricate. As noted in Section 3, diffraction limited diffractive telescopes are likely to have profiles with a minimum period of microns to mm—well within the capabilities of current micro-electro-mechanical systems (MEMS) or single point diamond turning (SPDT) technologies. Because the refractive index of the lens is so close to unity, the tolerances on the profile are comparatively relaxed. Even for the sub-nm wavelengths involved, lens figuring to $\lambda/10$ optical precision requires only $t_{2\pi}/10$ tolerances, where $t_{2\pi}$ is ~10–1000 μm (Figure 2). Radial tolerances for the same precision are no tighter than $p_{\min}/10$ and will usually be of a similar order of magnitude to the vertical tolerance.

Figure 3 shows that at energies greater than a few keV it is possible to select materials with N_0 greater than a few, meaning that not only is absorption of X-rays in the material forming the active part of a PZP or PFL small, but the profile can be etched or machined into a somewhat thicker substrate (or deposited onto one) without serious absorption losses.

Thus the profile can be close to ideal and losses can be small so, at least at their design energy, diffractive X-ray telescope lenses can have an effective area that is very close to their geometric area, which may easily be several square meters.

A great advantage of optical elements used in transmission rather than reflection is their relative insusceptibility to tilt errors and out-of-plane distortions. Multiple reflection mirror systems in which the radiation undergoes an even number of reflections, such as Wolter grazing incidence optics, are better in this respect than single reflection systems (provided the relative alignment of the mirrors does not change). However they still act as "thick" lenses and if the optic (or a part of it) is tilted by angle $\delta\psi$ the resulting transverse displacement of rays passing through it leads to an aberration in the image on angular scale $\sim (t/f)\delta\psi$, where t is the distance between the principal planes, a measure of the thickness of the "lens". For Wolter optics t is the axial distance between the centers of the two mirrors. For the Chandra optics $(t/f) = 0.08$. Diffractive telescope lenses are very close to ideal "thin" lenses, having (t/f) ratios of 10^{-6}–10^{-9} or even smaller.

4.2. Applications of High Angular Resolution Diffractive Telescopes. The most obvious attraction of diffractive optics for X-ray telescopes for astronomy is the potential they offer for superb angular resolution. From (3) it is apparent that angular resolution better than a milli-arcsecond should be readily obtainable in the X-ray band. With optics a few meters in size working with hard X-rays, sub-micro-arcsecond resolution should be possible.

One of the original incentives for the recent reconsideration of diffractive optics for high energy astronomy was indeed the possibility that it offers of sub-micro-arcsecond resolution. As has been discussed in proposals to use X-ray interferometry for astronomy [43, 44], this is the angular resolution that would be needed to image space-time around the supermassive black holes believed to exist at the centers of many galaxies. Even our own Galaxy, the Milky Way, apparently harbors a black hole, Sgr A*, with a mass of $4.3 \times 10^6\,\mathrm{M}_\odot$ (where $\mathrm{M}_\odot$ is the mass of the sun) [45].

The Schwarzschild radius of a black hole of mass M is

$$R_s = \frac{2GM}{c^2} = 2.9\frac{M}{\mathrm{M}_\odot}km, \tag{13}$$

where G is the gravitational constant and c the vacuum velocity of light. The radius of the "event horizon" is R_s in the case of a nonrotating black hole or somewhat larger for one with angular momentum. For Sgr A* R_s corresponds to an angular scale of 10 μ''. The black holes at the centers of "active" galaxies (Seyfert galaxies, Quasars and giant radio sources) can be much more massive—for example that in M87 may be as much as 2000 times the mass of Sgr A* [46]. Their Schwarzschild radii will be correspondingly bigger, so despite their much greater distances (also by a factor of 2000 in the case of M87), R_S in many cases still corresponds to angular scales of 0.1–10 μ''.

Of course one does not expect to detect radiation from the black hole itself, but the gravitational energy released by matter as it approaches the event horizon is the origin of the extremely high luminosity of some of these objects. Simulations have been made showing how such radiation originating near to the event horizon, even from behind the black hole itself, should appear after being bent by the gravitational field (Figure 7). The distribution expected depends not only on the mass of the black hole but on its angular momentum and inclination angle.

Figure 8 indicates the angular resolution available to astronomers with the current state of the art. At present the best angular resolution is obtained at mm wavelength by VLBI (very long baseline interferometry, see [47] for a recent review). Current technologies, with transatlantic

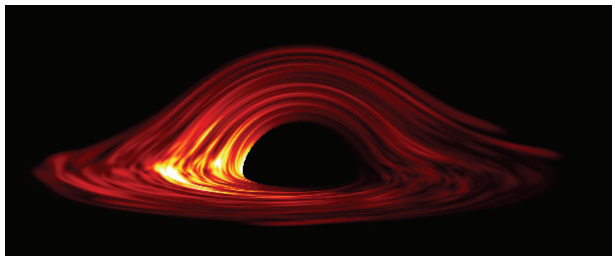

Figure 7: Simulation of X-ray radiation from the region surrounding a black hole. A Schwarzschild black hole is assumed to be seen at an inclination angle of 80°. For other details see Armitage and Reynolds [51].

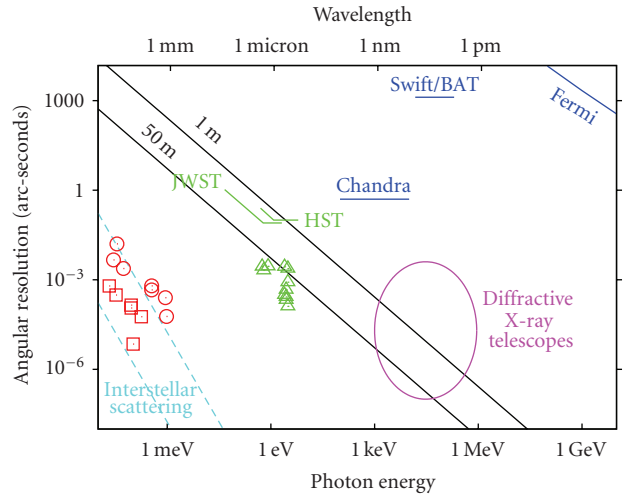

Figure 8: The angular resolution obtainable with different techniques and across the electromagnetic spectrum. The approximate domain in which diffractive X-ray optics are potentially of interest is indicated by an ellipse. Shown for comparison are (i) the Rayleigh limit for diffraction limited optics of 1 m and 50 m diameter (black lines), (ii) the angular resolution of current X-ray instruments (blues lines) and of the Hubble and James Webb Space Telescopes (green lines), (iii) the best resolution of some example optical interferometer systems (green triangles) and of some typical radio VLBI measurements (red circles), (iv) the diffraction-limited angular resolution possible with space VLBI (actual and near future; red squares), and (v) dashed lines (cyan) roughly indicating the region in which interstellar scattering becomes dominant at high galactic latitudes (left) and towards the galactic center (right). Note that while continuous lines refer to imaging instruments, the various symbols indicate the finest fringe spacing of interferometers which are not truly imaging.

baselines and wavelengths as short as 1 mm lead to angular resolutions down to 30–40 μ'', though so far only with a limited number of stations [48, 49], so a characteristic size is measured rather than forming an image. The Russian RadioAstron space VLBI mission, following in the footsteps of HALCA/VSOP, is due to be launched in 2011 and will extend baselines to 350,000 km, but the shortest wavelength is 13.5 mm. Although this should allow an angular resolution of 8 μ'', the actual resolution will be limited by interstellar scattering except at high galactic latitude. Consequently Sgr A* cannot be observed with the highest resolution. The Japanese-led Astro-G/VSOP-2 mission will go down to 7 mm in wavelength [50] and so be less affected by interstellar scattering (which is proportional to λ^2, as indicated by the dashed line in Figure 8), but with the maximum baseline limited by an apogee of only 25,000 km the best resolution will be 38 μ''. Astro-G launch has been delayed until at least 2013 due to technical problems with the deployable dish.

A useful basis of comparison across wavebands is the maximum baseline (or, for filled aperture instruments, the aperture diameter) in units of wavelength. Optical and infrared interferometers are pushing to higher and higher angular resolution, though as for VLBI, a limited number baselines provide sparse u–v plane coverage and allow model fitting, but only an approximation to true imaging. The 640 m and 330 m baselines of the SUSI and CHARA optical interferometers correspond to about 1.5 Gλ and 0.7 Gλ, respectively, while with radio VLBI fringes have been obtained with baseline as long as 6 Gλ [52]. A modest 1 m diameter lens working with 6 keV X-rays would have a size of 50 Gλ, and larger lenses and those working at higher energies have corresponding greater values. In addition such lenses would provide full u–v plane coverage up to this scale.

It is ironical that in the X-ray and gamma-ray bands, where the wavelengths are shortest and diffraction least limiting, the angular resolution at present obtainable is actually inferior to that possible at longer wavelengths. No currently planned X-ray mission will improve on, or even equal, the 0.5″ resolution of the Chandra grazing incidence mirror. While being subject to some constraints and limitations, discussed below, in appropriate circumstances diffractive optics offer the opportunity of improvements by up to 6 order of magnitude. X-ray imaging may then move from the present arc-second domain to the milli-arcsecond one, where stellar surfaces can be imaged and the formation of astrophysical jets examined in detail, and to micro-arcseconds, the resolution needed for black hole imaging.

4.3. Applications of Diffractive Optics for Light Buckets. Even if one does not take advantage of the imaging capabilities of diffractive X-ray optics, they may prove useful as flux concentrators. X-ray and gamma-ray astronomy is limited both by the small number of photons often detected and by background in the detector, mostly due to particles. The background is typically proportional to the detector area from which events are accepted. Catching photons requires large collecting area, whereas reducing background implies that the detector should be as small as possible. Applications of X-ray "light buckets" optimized for these purposes include high-resolution spectroscopy and fast timing measurements with moderate energy resolution such as studies of quasi-periodic oscillations, allowing the observation of certain general relativity effects such as frame dragging in compact black hole binaries.

At the energies where they can be used, grazing incidence reflective optics offer a solution to the problem of how to concentrate the flux from a large collecting area onto a small

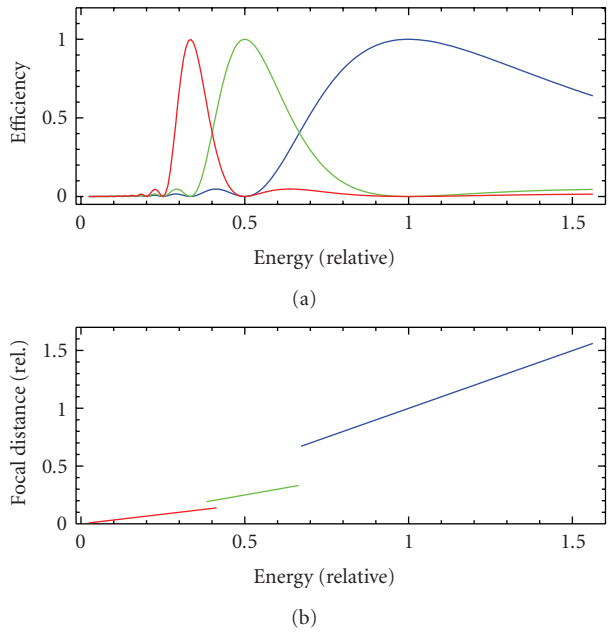

FIGURE 9: A PFL will work with relatively high efficiency over a broad band of energies provided that the detector plane is moved to the appropriate distance. The blue curve corresponds to the lens operating in the nominal mode. For the green and red curves the detector is assumed to be placed at the distances for the focii of the lens treated as a $t_{4\pi}$ and $t_{6\pi}$ one. Higher-order responses are not shown. Absorption effects are not taken into account in the plots based on [30].

detector area. Diffractive optics provide an alternative to grazing incidence mirrors—one that can be used even for high energies, and indeed whose performance is in many respects best at high energies.

For a concentrator one can drop the requirement of being able to resolve with the detector a spot size corresponding to the diffraction-limited angular resolution of which the optic might be capable. Smaller $p_{\min}$ may be used and so the focal length reduced. From the same geometric considerations that lead to (7), the bandwidth will be

$$\frac{\Delta E}{E} = 2\left(\frac{d_{\text{det}}}{d}\right), \tag{14}$$

whereas, assuming ideal efficiency for the optic and the detector, the flux is concentrated by a factor

$$C = \frac{A_{\text{eff}}}{A_{\text{det}}} \approx \left(\frac{d}{d_{\text{det}}}\right)^2 \approx 4\left(\frac{E}{\Delta E}\right)^2. \tag{15}$$

Thus where narrow spectral lines, or groups of lines, from a compact source are to be studied, significant advantages are available.

5. Overcoming the Difficulties

5.1. Minimizing Chromatic Aberration. Minimizing the effects of chromatic aberration is one of the biggest challenges to overcome in developing diffractive X-ray telescopes. The various measures that can be taken are discussed below.

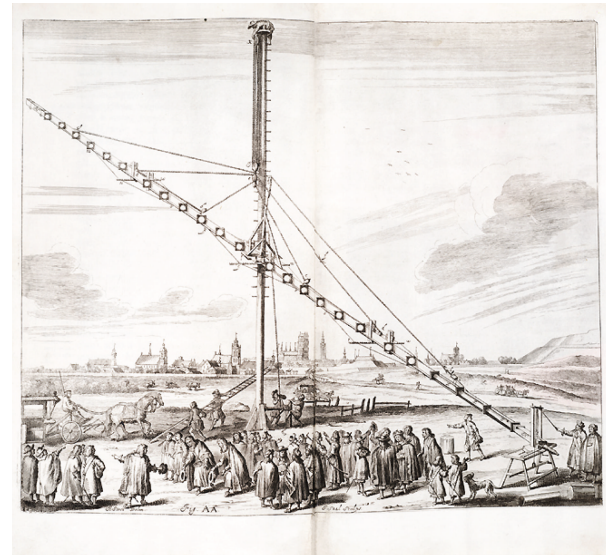

FIGURE 10: It has long been known that chromatic aberration is minimized by adopting a long focal length. Before the invention of the achromatic lens Hevelius built telescopes with 60 and (shown here) 140 foot focal lengths [53].

5.1.1. Refocusing. The first thing to note is that a diffractive X-ray lenses can work well over a broad range of energies provided the detector position is adjusted for each energy. Figure 9 shows the effective area of a PFL as a function of energy *if the telescope is refocused by adjusting the detector plane to the optimum position for each energy*. Braig and Predehl have pointed out [29] that, as indicated in the figure, well below the energy, E_0 for which a PFL was designed one can take advantage of the high efficiency near $E_0/2$, $E_0/3, \ldots$ because the lens acts like a $t_{4\pi}$, $t_{6\pi} \ldots$ one in the sense described in Section 3.2. As only one energy can be observed at a time this is not a very practical way of making broadband observations, but the approach could be useful in studying, for example, lines whose energy may be red-shifted to different extents in different sources. Note that at energies where the efficiency is less than unity, the lost flux appears in focii of other orders. The resulting halo to the PSF will have low surface brightness compared with the peak, but if it is troublesome it is possible to imagine blanking off the inner part of the lens area [29].

5.1.2. Improving Chromatic Aberration with Long Focal Lengths. From (7) it is clear that the effect of chromatic aberration on angular resolution is reduced if the focal ratio is large. For a given lens size, this means that the focal length should be as long as is consistent with other constraints. This is a long-known effect; before the invention of the (visible-light) achromatic doublet, astronomical telescopes were built with very long focal lengths in order to minimize chromatic aberration. Figure 10 shows an extreme example. Long focal lengths lead to a limited field of view (Section 5.4) and tend to have severe implications for the logistics of

maintaining the telescope in space (Section 5.2), but the bandwidth increases in proportion to f.

5.1.3. Segmenting Lenses for Multienergy Operation. Given that PFLs of large surface area are not too difficult to make but wide bandwidth is hard to achieve, it has been pointed out on a number of occasions (e.g., [26, 28, 29]) that the surface of a diffractive lens can be divided into regions tuned to different energies, thus providing information over a wider bandpass. The division may be into a few zones or into many, and an aperture may be divided radially or azimuthally, or both. The "subtelescopes" so formed may be either concentric, or parallel but offset.

An important consideration is the interference fringes that are produced when radiation of the same energy arrives in the same part of the detector after passing through the different regions of the diffractive optic, including those designed for quite different energies. In some of the work of Braig and Predehl [30, 54, 55] this issue is avoided by assuming, explicitly or implicitly, that the lens is made from many small segments that are subject to random position deviations such that their outputs add incoherently rather than coherently. In this case the resolution is of course that associated with the characteristic size of a segment (e.g., a few centimeters) rather than the lens as a whole (e.g., a few meters).

5.1.4. Diffractive-Diffractive Correction. In some circumstances the dispersion of a diffractive optical element can be corrected using that of a second diffractive optical element. However, as shown formally by Bennett [56] no optical system consisting of only two diffractive lenses can form a real image, free from longitudinal dispersion, from a real object. Buralli and Rogers [57] generalized this result to any number of diffractive elements. Michette et al. [58] has described some schemes that get around this constraint, but they do so only by allowing diffraction into multiple orders with a consequent loss in efficiency and they only provide correction at two disparate energies. Other optical systems that do correct one dispersive element with another either involve virtual images (or objects), or depend on reflective (or refractive) relay optics. The space-based visible light diffractive imager proposed by Koechlin et al. [59] is an example of the use of reflective relay optics.

X-ray telescopes that depend on both diffractive and reflective optics risk suffering the disadvantages of both, so correction schemes that depend on reflective relay optics do not seem very attractive. On the other hand, as will be noted below (Section 5.2), there are perhaps other reasons for considering incorporating a reflective component, so perhaps a feasible diffractive-reflective-diffractive design may eventually evolve.

5.1.5. Diffractive-Refractive Correction. Given the constraints that apply to diffractive-diffractive correction for telescopes forming real images, the possibility of correction using refractive optics has been widely considered. The constraints

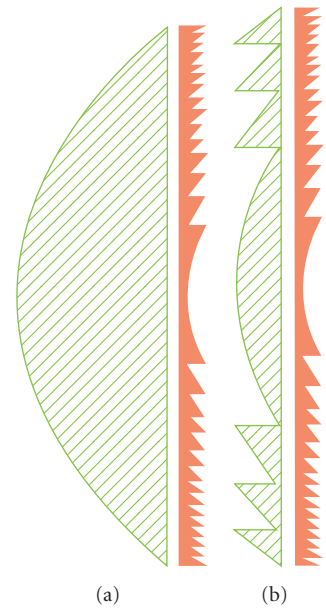

Figure 11: (a) the use of a refractive X-ray lens to chromatically correct a diffractive one. (b) A more practical configuration in which the refractive component is stepped to reduce absorption.

that preclude achromatic correction of one diffractive element with another arise because the dispersion of the two elements would be the same. Correction of a diffractive lens with a glass one is used in the visible part of the spectrum where glasses have a dispersion that differs from the E^{-1} dependence of the power of diffractive elements (e.g., [62]). The same principle can be applied to X-rays—purely refractive lenses can be made [63] and are widely used in X-ray microscopy and beam manipulation, often stacked to provide adequate power. Figure 2 shows that for most materials over most of the X-ray band $t_{2\pi}$ is proportional to E, implying that the power of a refractive lens, which depends on δ, is proportional to E^{-2}.

Figure 11, shows how in principle first-order correction of longitudinal chromatic aberration of a PFL (or ZP, PZP) is possible with a diffractive/refractive X-ray doublet [26, 27, 60]. Because the lens remains a "thin" one, there is almost no lateral color aberration. In the common situation where $t_{2\pi}$ is proportional to E, the focal length of the refractive component should be $-2f_d$, where f_d is that of the diffractive one, and the combined focal length is $2f_d$. In this case the number of Fresnel zones in the refractive component is half the number in the PFL. In the absence of absorption the bandpass is increased from $\Delta E/E = 1/N_F$ (11) to $\Delta E/E = 1/\sqrt{N_F}$ (e.g., [64]) (here N_F is the number of Fresnel zones in a single lens having the focal length of the combination).

It has already been noted (Section 3.5) that absorption becomes important in a refractive lens if N_z exceeds the critical Fresnel number N_0 for the material. As in practice N_0 is usually a few tens up to a few hundred (Figure 3), this sets a limit on the size of diffractive lens that can be corrected this way. Wang et al. [65] have suggested using the rapid energy dependence of δ just above absorption

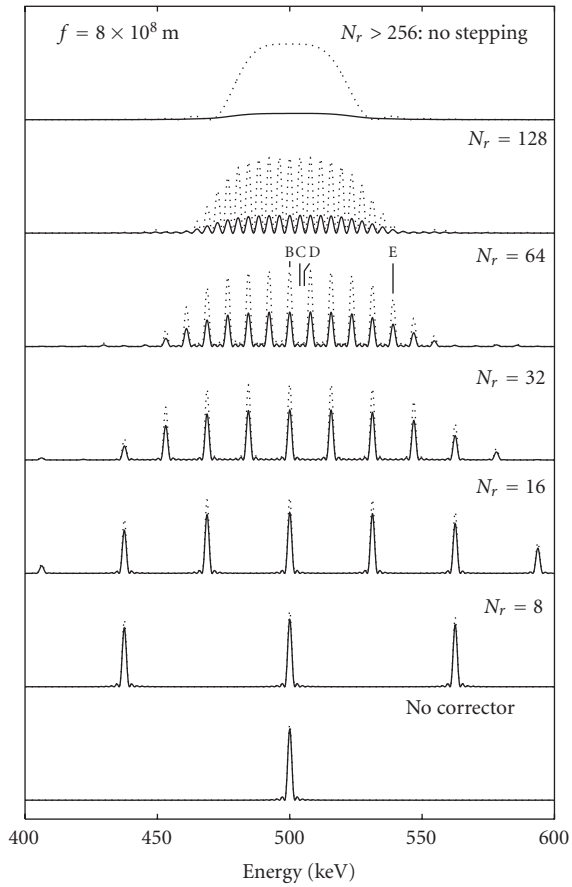

FIGURE 12: Simulated response of a refractive/diffractive achromatic doublet with different degrees of stepping of the refractive component. N_r corresponds to m in the text. The dotted lines indicate the response if there were no absorption. As the step size is made smaller, the density of coverage within the bandpass becomes worse but the effects of absorption become less serious and the band covered becomes wider, details in [60], from which this figure is taken.

edges to reduce the thickness of the refractive component needed. This approach only works at very specific energies, but it could make possible achromatic diffractive-refractive doublets several millimeters in diameter for microscopy and microlithography.

A PFL can be considered as a refractive lens in which the thickness is reduced Modulo($t_{2\pi}$). Thus it is natural to consider reducing the absorption in a refractive correcting lens by stepping it back, not Modulo($t_{2\pi}$) which simply would make it another PFL, but Modulo($m\ t_{2\pi}$) for some large integer m as in Figure 11. $t_{2\pi}$ varies with energy, so the value at some particular energy, E_0, must be chosen. Coherence is then maintained across the steps at this energy and at any other for which $m'[t_{2\pi}(E)] = m\ [t_{2\pi}(E_0)]$ for some other integer m'. This occurs at a comb of energies. In the regime where $t_{2\pi}$ is proportional to E, they occur at intervals such that $\Delta E/E \sim 1/m$. Detailed analyses of the response of PFLs with stepped achromatic correctors have been published [55, 60]. Examples are shown in Figure 12. As the step size is made smaller and the number of zones N_Z within the refractive component increases, the density of coverage within the bandpass decreases as N_Z^{-1} and the band covered becomes wider (improving approximately as $N_Z^{1/2}$) and the effects of absorption become less serious.

If one is willing to consider configurations involving the alignment of not just two widely spaced components, but three, then the configuration indicated in Figure 13 offers an even wider bandpass (see [28] and references therein; more details are provided in [60]). With the extra degree of freedom introduced by the separation between the two lenses it is possible to set to zero not just dz/dE (z being the axial position of the image), but also d^2z/dE^2. The bandwidth is increased as indicated in Table 3. The fact that the image is somewhat magnified compared with a single lens system of the same overall length could be advantageous. However as the magnification is energy dependent, care must be taken that lateral chromatic aberration does not limit the useful field of view (this will not be a problem if the detector has adequate energy resolution to allow post-facto scale-factor correction).

5.1.6. Axicons, Axilenses, and Other Wideband Variants. Variations of the ZP have been proposed in which the shape of the PSF is modified to (slightly) improve the angular resolution (e.g., [68]) or in the case of "photon sieves" to improve the resolution available with a given minimum feature size in the fabrication [69]. One such variant, the "fractal photon sieve" has been shown to have an extended spectral response [70], achieved because some of the power from the prime focus is diverted into focii at other distances. As will be seen below, this can be accomplished in other more controlled and efficient ways.

A diffractive lens can be considered as a circular diffraction grating in which the pitch varies inversely with radius so that radiation of a particular wavelength is always diffracted towards the same focal point. Regarded in this way, a PFL is a variable pitch phase grating, blazed in such a way that all of the energy goes into the +1 order. Skinner [66, 71] has discussed the application to X-ray telescopes of designs in which the pitch varies radially according to laws other than r^{-1}. They can be considered as forms of radially segmented lenses in which the pitch varies smoothly rather than in steps.

In an extreme case the pitch is constant and one has the diffractive X-ray axicon. Interestingly, to a first approximation the point source response function of an axicon is independent of energy. According to the Rayleigh criterion, the angular resolution is similar to that of a PFL of the same diameter working at the lowest energy, but the secondary diffraction rings are stronger so the HPD is larger. Indeed over a wide range of radii the PSF shape is such that the enclosed power simply increases, approximately linearly, with radius. In some respects the system should be regarded as an (achromatic) interferometer in which the information is contained more in the fringes than in the central response.

Intermediate designs are possible in which the bandpass is tailored to particular requirements based on the ideas of Sochacki [72] and of Cao and Chi [73]. This leads to the diffractive X-ray axilens discussed in [66]. The bandwidth

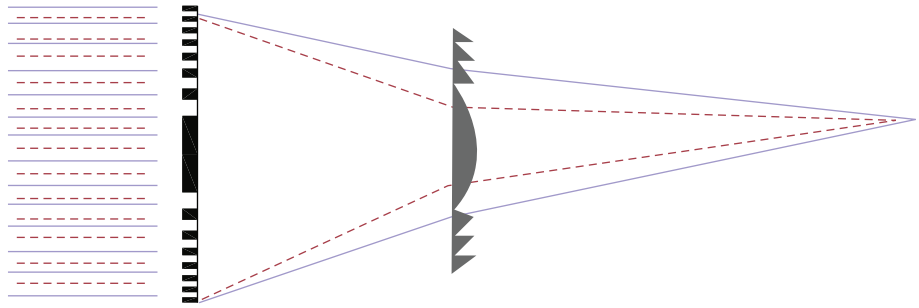

Figure 13: A variation on the refractive/diffractive achromatic doublet shown in Figure 11 in which the components are separated, allowing second-order correction of longitudinal color (Figure from [61]). A stepped version of the refractive component is shown.

Table 3: Achromatic correction of PFLs. Parameters are given for systems with the same overall length, f, at the nominal design energy, E_0, and for the case when $t_{2\pi}$ is proportional to energy, E. In the table ΔE is specified relative to E_0, and d is the diameter of the refractive component.

	Simple PFL	Doublet	Separated pair
Diffractive focal length	f	$f/2$	$f/3$
Separation	—	0	$f/9$
Refractive focal length	—	$-f$	$-8/27f$
Image plane distance	$f(1+\Delta E)$	$f(1+\Delta E^2+\cdots)$	$f(1+1.35\Delta E^3+\cdots)$
Image scale	f	f	$\frac{4}{3}f(1-(1/2)\Delta E+\cdots)$
Diffraction-limited bandwidth (fractional)	$4((f/d^2)(hc/E))$	$4((f/d^2)(hc/E))^{1/2}$	$((16/3)(f/d^2)(hc/E))^{1/3}$

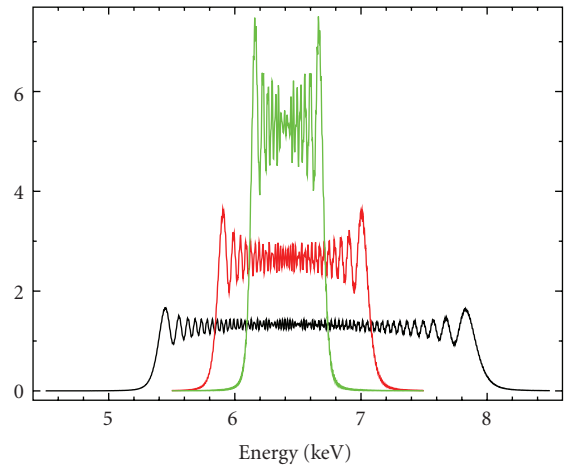

Figure 14: The on-axis response as a function of photon energy at a fixed distance of 100 m for Axilenses with different parameters [66].

can be selected at will; Figure 14 shows the response of some examples. For diffraction-limited operation, the area-bandwidth product tends to be no greater than that of a narrow band PFL. As the later has the advantage that the detector noise within a narrow band is small, devices of the axicon/axilens family are most likely to find application where an extended bandpass is essential, for example in order to include the whole of a broadened line or a group of lines.

5.1.7. Figures of Merit. Braig and Predehl [64] define an "Achromatic Gain" parameter $\mathcal{G}$ to measure the advantage that an achromatic system has over a simple lens. It is essentially the ratio of the effective areas, integrated over the energy range in the two cases.

The achromatic gain $\mathcal{G}$ may be generalized to quantify the advantage compared to a simple PFL of other variants as well as of achromatic combinations. As neither the resolution nor the image scale are necessarily the same in all cases, it is best to base the effective area on the flux within a diffraction-limited focal spot rather than peak brightness. Such a figure of merit was used in [71] where it was shown that axicons and axilenses have a "$\mathcal{G}$" close to unity—the extra bandwidth is obtained at the expense of effective area. The same is obviously true if a lens is segmented into areas devoted to different energies. On the other hand increasing the focal length is accompanied by an increase in bandwidth (11) and of $\mathcal{G}$.

Care must be used in interpreting this parameter. It measures the (square of) the improvement in signal-to-noise ratio on the assumption that the noise is dominated by photon statistics from the source. If the observation is dominated by detector background that is not source related, such as that due to particles, then a dependence on the square root of the bandwidth would be more appropriate. This assumes that the passband of the optic is wider than the energy resolution of the detector. In the detector background limited case, the background will also depend on the detector area over which the signal is spread, or on the area of a spot size dictated by the detector resolution if that is larger. Furthermore, by considering only the central spot, the information carried by the flux in high amplitude sidelobes such as occur in the PSF of axicons and axilenses, is ignored.

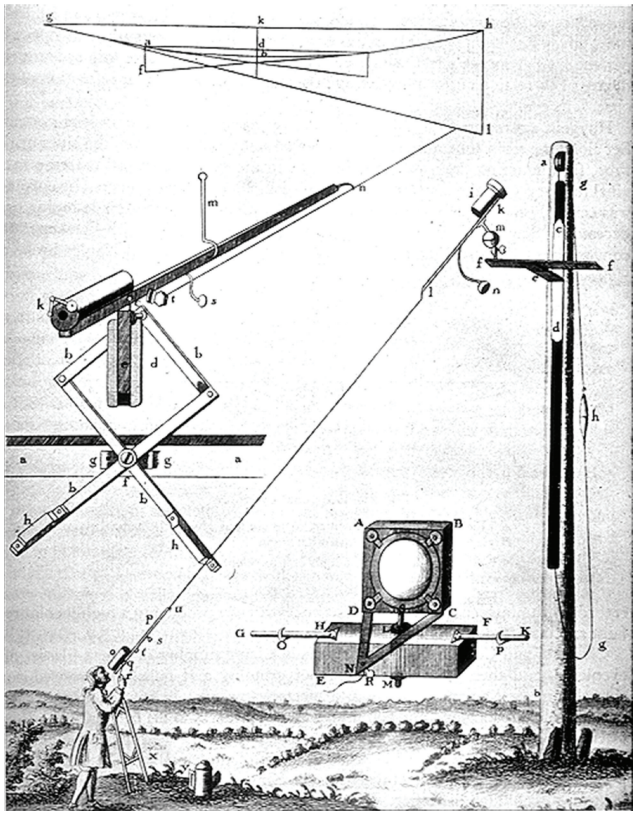

Figure 15: The concept of a telescope in which the objective of a telescope and the detector are not rigidly connected is not new. Christian Huygens (1629–1687) used this 210 foot focal length telescope [67]. Note that the design takes advantage of the relative immunity of a thin lens to tilt errors.

5.2. Focal Length: Formation Flying. Equation (2) makes it clear that the focal length, f, of any practical system is likely to be long, particularly at high energies. In addition in various respects discussed above, *very* large f will often give the best performance.

First, in Section 3.1 it was seen that a minimum focal length is required if spatial resolution of a detector at the prime focus is not to be a limiting factor. For example, even if the detector pixels are as small as 10 μm a resolution of 1 μ'' implies $f > 2000$ km. Gorenstein [74] has suggested that this problem might be alleviated if a grazing incidence reflecting telescope were used to reimage the prime focus, perhaps with a magnification by a factor of 20. Radiation from a particular sky pixel would in practice illuminate a very small part of the telescope surface because the latter would be very close to the focal plane. The reflecting surface would in effect remap positions over its aperture to pixels in a detector plane.

A second reason that long f may give the best performance is that as noted in Section 5.1 chromatic aberration is minimized if f is long.

Finally, based on (2), unless f is large diffractive lenses of a reasonable size will have a very small period $p_{\min}$ and fabrication will be more difficult and perhaps less precise.

For focal lengths of up to ~100 m, it is perhaps possible to consider telescopes with a boom connecting the lens and the detector assembly. Deployable booms of up to 60 m have been flown in space [75]; the record for the largest rigid structure in space is now held by ISS at over 100 m. On the other hand even for a focal length of 50 m, ESA studies for the proposed XEUS grazing incidence mirror X-ray mission concluded that a boom was unnecessary and that formation flying of separate spacecraft carrying the optic and the detector assemble offered a more viable solution [76]. It is interesting that a telescope without a rigid connection between objective and detector is not a new concept—see Figure 15.

Formation flying for a long focal length telescope mission implies maintaining two spacecraft such that the line joining them has a fixed direction in inertial space. Because of gravity gradients within the solar system, as well as disturbances such as those due to differences in solar radiation pressure, a continuous thrust will be needed on at least one spacecraft. Another consideration is that a major repointing of the telescope will require maneuvering one of the spacecraft by a distance $\sim f$.

Some of the issues associated with formation flying of two spacecraft for a diffractive X-ray telescope mission have been briefly discussed in the literature [25, 29]. Internal studies at NASA-GSFC's Integrated Mission Design Center of possible missions based on this technique have considered the issues more deeply. Krizmanic et al. [77] has reported on one of these and updated some of the conclusions. The missions studied were considered ambitious, but possible. A single launcher would launch both lens and detector spacecraft either to the vicinity of the L2 Lagrangian point or into a "drift-away" orbit around the sun. Existing ion thrusters can provide the necessary forces both to maintain the pointing direction against gravity gradient forces and disturbances and for reorienting the formation. The fuel and power needed for the thrusters are acceptable. In short, no "show stoppers" were identified.

5.3. Pointing Knowledge. Although precise control of the *distance* between lens and detector is not needed, the knowledge of the *direction* in celestial space of their vector separation is crucial. As information about every photon detected can be time tagged, *control* is needed "only" to the extent necessary to ensure that the image of the region to be studied falls on the detector area (Section 5.4). *Knowledge* of the orientation is needed, however, to a level corresponding to the angular resolution required. This amounts to a need to establish the transverse position of the detector with respect to a line passing from the source through the center of the lens, and to do so with a precision that can be from a millimeter down to a few microns.

The problem of precise attitude determination in celestial coordinates is one common to all missions attempting to work at the milli-/micro-arcsecond level. It has already been considered in the context of the studies of MAXIM, a proposed mission to address the problem of imaging space-time around black holes using X-ray interferometry. Gendreau et al. reviewed a number of approaches to the problem [78]. If a laser beacon is placed on the lens spacecraft and viewed against background stars, a "super-startracker"

on the detector spacecraft can in principle provide the necessary information. Obtaining measurements with the necessary precision is not out of the question—astrometry is already in an era where milli-arcsecond accuracy is the norm and micro-arc-second the target. The problem is obtaining that precision with faint stars on short enough time scales. Fortunately various technologies discussed by Gendreau et al. offer the prospect of gyroscopic systems that would have sufficient precision to allow interpolation between absolute fixes from the stellar observations. To further alleviate the difficulties, Luquette and Sanner [79] have discussed how knowledge of the dynamics dictating the spacecraft displacements can help with determining short term changes to the alignment.

5.4. Field of View. The fields of view of ultrahigh angular resolution telescopes such as those possible using diffractive optics are necessarily limited. With a single lens configuration, or with a contact achromatic doublet, the field of view will simply be the detector size divided by the focal length. With long focal lengths, reasonable detector sizes imply small fields of view. Although optical systems with separated lenses (Section 5.1.5) or with relay mirrors (Section 5.2) can change the image scale, this would probably be in the sense of increasing it, so reducing the field of view.

There is, anyway, a basic limitation. If for example micro-arc-second resolution was wanted over a 1" field of view, a detector with $>10^{12}$ pixels would be needed. The present state of the art for X-ray detectors in space is indicated by a few examples. The EPIC camera on XMM-Newton has an array of 7 CCDs with a total of 2.5×10^6 pixels. The imaging array of the ACIS focal plane instrument on Chandra has 4×10^6 pixels in 4 CCDs. Although the e-Rosita telescopes will have a total area of CCDs about an order of magnitude greater than present generation X-ray instruments, the pixel size will be larger to match the telescopes and the number of pixels will be only just over 10^6 [80]. Instruments planned for the IXO X-ray observatory are also in the few megapixel range, though a single monolithic device will cover 100 cm^2 [81].

Larger arrays of larger format CCDs are possible. Although the requirements are a little different for visible radiation, ESA's Gaia astrometry mission will have an array of 106 CCDs covering about half a square meter, with $\sim 9 \times 10^8$ pixels [82]. The Gaia pixels are rectangular 20×30 μm. Taking 20 μm as a typical dimension, a similar array would provide a field of view 30 milli-arc-seconds across with 1 μ'' pixels at a focal distance of just over 4000 km.

Of course, even where a 10^{12} pixel detector is available, it would require an extremely strong source to produce a significant signal in even a small fraction of the pixels. Sources of interest for study at the resolution possible with diffractive X-ray optics are necessarily rather compact.

6. Alternatives to Simple Lenses

Equation (3) implies that sub-micro-arcsecond angular resolution should be possible with modest sized lenses working at a few hundred keV. There is a special interest, though, in such measurements in the X-ray band. Not only are the photons more numerous, but the emission spectra of AGN typically show strong emission lines in the region of 6.7 keV associated with highly ionized Fe. These lines carry important diagnostic information because they are shifted in energy both by gravitational redshifts and by the Doppler effect. Ultra-high angular resolution mapping at energies in this band would be particularly valuable but would require lenses 50 m or more in diameter.

Although membrane/unfoldable Fresnel lenses of 25–100 m diameter for visible light have been proposed [83] and even been demonstrated on the ground on scales of up to 5 m [84], X-ray lenses of this size would not be easy to engineer and would actually have an effective area larger than needed from the point of view of photon flux.

A PFL with a partially filled aperture can be envisioned. It could comprise subsections of a PFL mounted on multiple spacecraft distributed over a plane [66, 85]. The system then becomes somewhat similar to that proposed within the studies of the proposed MAXIM (Micro-Arcsecond-X-ray IMager) mission in which mirror assemblies on spacecraft distributed over a plane would divert radiation to form fringes on a detector situated at a large distance [86]. In both cases tight control of the distances of the spacecraft from the center of the array would be needed (to a fraction of $p_{\min}$ for the partially filled PFL; similar for a MAXIM formation of the same size). The differences are (1) that the subsections of a partially filled aperture PFL would concentrate flux, whereas the plane mirrors proposed for MAXIM would not and (2) mirror reflection is achromatic, whereas the PFL subsections would divert radiation by a wavelength-dependent angle and fringes would only be formed where the concentrated, deflected, beams cross. The bandwidth over which fringes appear can be improved by altering the radial dependence of the pattern pitch in the PFL in ways analogous to X-ray axicons and axilenses. In the constant pitch (axicon) case one has a MAXIM-like interferometer in which the beam diverters are blazed diffraction gratings, and the borderline between imaging and interferometry becomes blurred.

7. Conclusions: Status and Prospects

As mentioned in the introduction, diffractive X-ray telescopes presently exist almost entirely as concepts and proposals on paper. Some work has been conducted on verifying that no problems exist and on demonstrating feasibility using scaled systems [87] fabricated by gray scale lithography [88]. By scaling down in radius (but not in thickness) the form of a large PFL that might be used for astronomy, the focal length is reduced. Lenses a few mm in diameter and with a focal length of ~100 m can act as models of ones, say, a few meters in diameter for which $f \sim 100$ km. With this reduced focal length testing is possible using existing ground-based facilities such as the 600 m long X-ray interferometry testbed at NASA-GSFC [89, 90]. Ironically the smaller lenses are *more* difficult to make than a flight lens would be, because the period of the profile is correspondingly reduced.

Tests and developments of small-scale PFLs, using various fabrication techniques and including achromatic combinations are continuing [91]. Progress to a micro-arcsecond mission would probably be through an intermediate level "pathfinder mission". Braig and Predehl [55] have suggested a concept in which a 3.5 m lens is divided radially into two regions operating, respectively, at 5 and 10 keV. Each would be made from many small achromatic segments whose outputs are assumed to add incoherently so the angular resolution is ~1 milli-arcsecond. Note that the proposed use of Lithium for the 5 keV component is unlikely to be practicable due to fabrication difficulties and to oxidation.

A specific proposal for a pathfinder mission, MASSIM [92], operating in the milli-arcsecond regime has been made in the context of NASA's "Advanced Mission Concept Studies". With a focal length of 1000 km, MASSIM would provide sub-milli-arc-second resolution with an effective area of 2000–4000 cm^2 over a pseudo-continuous 5–11 keV band using five 1 meter diameter achromatic lenses. MASSIM would allow important scientific objectives to be achieved, in particular allowing the imaging of the inner regions of jets where the acceleration takes place, while at the same time providing a stepping stone to an eventual micro-arc-second mission. It requires two spacecraft, one station keeping with respect to the other another to a fraction of a meter. A major technology driver would be the determination of direction of the actual line of sight with an accuracy corresponding to the target resolution. The proposed pointing determination method involves a state-of-the-art startracker on the detector spacecraft viewing the sky and simultaneously a beacon on the spacecraft carrying the lenses.

Another possible route forward is through solar imagery where even small diffractive lenses, little larger than those already demonstrated and having modest focal lengths (<100 m), could provide images of Fe line emission ~6.7 keV from active regions with an angular resolution many times better than any yet achieved.

In conclusion, diffractive optics offer a new family of possibilities for telescopes. Despite drawbacks in terms of inconvenient focal lengths and limited field of view and bandwidth, the potential that they have for flux concentration even at high energies and, in particular, for superb angular resolution suggests that in due course they will find their place in the range of techniques available to X-ray and gamma-ray astronomy.

Acknowledgments

The author wishes to thank colleagues for helpful discussions and in particular John Krizmanic for a careful reading of the paper and for useful suggestions.

References

[1] P. Gorenstein, "Focusing X-ray optics for astronomy," *X-Ray Optics and Instrumentation*, vol. 2010, Article ID 109740, 2010.

[2] R. Petre, "Thin shell, segmented X-ray mirrors," *X-Ray Optics and Instrumentation*, vol. 2010, Article ID 412323, 2010.

[3] M. Bavdas, M. Collon, M. Beijersbergen, K. Wallace, and E. Wille, "X-ray pore optics technologies and their application in

space telescopes," *X-Ray Optics and Instrumentation*, vol. 2010, Article ID 295095, 2010.

[4] L. Mertz, *Transformations in Optics*, John Wiley & Sons, New York, NY, USA, 1965.

[5] D. T. Wilson, G. D. DeMeester, H. H. Barrett, and E. Barsack, "A new configuration for coded aperture imaging," *Optics Communications*, vol. 8, no. 4, pp. 384–386, 1973.

[6] U. D. Desai, J. P. Norris, and R. J. Nemiroff, "Soft gamma-ray telescope for space flight use," in *Astroparticle Physics and Novel Gamma-Ray Telescopes*, D. B. Cline, Ed., vol. 1948 of *Proceedings of SPIE*, pp. 75–81, Orlando, Fla, USA, April 1993.

[7] F. Frontera and P. von Ballmoos, "Laue gamma-ray lenses for space astrophysics: status and prospects," *X-Ray Optics and Instrumentation*, vol. 2010, Article ID 215375, 2010.

[8] R. W. Wood, *Physical Optics*, Macmillan, New York, NY, USA, 3rd edition, 1934.

[9] J. Kirz, "Phase zone plates for X rays and the extreme UV," *Journal ofthe Optical Society of America*, vol. 64, no. 3, pp. 301–309, 1974.

[10] J. L. Soret, "Ueber die durch Kreisgitter erzeugten Diffractions phanomene," *Annalen der Physik*, vol. 232, pp. 99–113, 1875.

[11] L. Rayleigh, "Encyclopedia Britannica".

[12] R. W. Wood, "Phase reversal zone plates and diffraction telescope," *Philosophical Magazine*, vol. 45, p. 511, 1898.

[13] K. Miyamoto, "The phase Fresnel lens," *Journal of the Optical Society of America*, vol. 51, no. 1, pp. 17–20, 1961.

[14] O. E. Myers, "Studies of transmission zone plates," *American Journal of Physics*, vol. 19, pp. 359–365, 1951.

[15] A. V. Baez, "A study in diffraction microscopy with special reference to X-rays," *Journal of the Optical Society of America*, vol. 42, no. 10, p. 756, 1952.

[16] G. Elwert, "X-ray picture of the sun taken with fresnel zone plates," in *Structure and Development of Solar Active Regions*, K. O. Kiepenheuer, Ed., vol. 35 of *IAU Symposium*, pp. 439–443, 1968.

[17] H. Bräuninger, H. J. Einighammer, J. V. Feitzinger et al., "EUV and soft X-ray images of the sun on March 11th, 1971," *Solar Physics*, vol. 20, no. 1, pp. 81–84, 1971.

[18] M. Burger and J. H. Dijkstra, "Photographs of the Sun in the XUV-region," *Solar Physics*, vol. 24, no. 2, pp. 395–404, 1972.

[19] J. H. Dijkstra, W. de Graaff, and L. J. Lantwaard, "Construction of apodised zone plates for solar X-ray image formation," in *New Techniques in Space Astronomy*, F. Labuhn and R. Lust, Eds., vol. 41 of *IAU Symposium*, pp. 207–210, 1971.

[20] G. Elwert and F. Feitzinger, "The image improvement of field-sources with zone plates, especially of the sun in the XUV and soft X-region," *Optik*, vol. 6, pp. 600–612, 1970.

[21] R. Giacconi, W. P. Reidy, T. Zehnpfennig, J. C. Lindsay, and W. S. Muney, "Solar X-ray image obtained using grazing-incidence optics," *The Astrophysical Journal*, vol. 142, pp. 1274–1278, 1965.

[22] G. S. Vaiana, L. van Speybroeck, M. V. Zombeck, A. S. Krieger, J. K. Silk, and A. Timothy, "The S-054 X-ray telescope experiment on SKYLAB," *Space Science Instrumentation*, vol. 3, no. 1, pp. 19–76, 1977.

[23] B. Niemann, *Investigations of zone plate telescopes for the use of non-solar sources in the range of soft X-radiation*, Ph.D. thesis, Mathematisch-Naturwissenschaftliche Fakultät, Gottingen University, Germany, 1974.

[24] D. Dewey, T. H. Markert, and M. L. Schattenburg, "Diffractive-optic telescope for x-ray astronomy," in *Multilayer and Grazing Incidence X-Ray/EUV Optics III*, vol. 2805 of *Proceedings of SPIE*, pp. 224–235, Denver, Colo, USA, August 1996.

[25] G. K. Skinner, "Diffractive/refractive optics for high energy astronomy. I. Gamma-ray phase Fresnel lenses," *Astronomy and Astrophysics*, vol. 375, no. 2, pp. 691–700, 2001.

[26] G. K. Skinner, "Diffractive-refractive optics for high energy astronomy II. Variations on the theme," *Astronomy and Astrophysics*, vol. 383, no. 1, pp. 352–359, 2002.

[27] P. Gorenstein, "Concepts: X-ray telescopes with high angular resolution and high throughput," in *X-ray and Gamma-Ray Telescopes and Instruments for Astronomy*, J. E. Truemper and H. D. Tananbaum, Eds., vol. 4851 of *Proceedings of SPIE*, pp. 599–606, Waikoloa, Hawaii, USA, August 2002.

[28] P. Gorenstein, "Role of diffractive and refractive optics in x-ray astronomy," in *Optics for EUV, X-Ray, and Gamma-Ray Astronomy*, O. Citterio and S. L. O'Dell, Eds., vol. 5168 of *Proceedings of SPIE*, pp. 411–419, San Diego, Calif, USA, August 2004.

[29] C. Braig and P. Predehl, "X-ray astronomy with ultra-high angular resolution," in *UV and Gamma-Ray Space Telescope Systems*, G. Hasinger and M. J. L. Turner, Eds., vol. 5488 of *Proceedings of SPIE*, pp. 601–612, Glasgow, UK, June 2004.

[30] C. Braig and P. Predehl, "Large-scale diffractive X-ray telescopes," *Experimental Astronomy*, vol. 21, no. 2, pp. 101–123, 2006.

[31] D. J. Stigliani Jr., R. Mittra, and R. G. Semonin, "Resolving power of a zone plate," *Journal of the Optical Society of America*, vol. 57, pp. 610–611, 1967.

[32] W. Chao, E. H. Anderson, P. Fischer, and D. -H. Kim, "Towards sub-10 nm resolution zone plates using the overlay nanofabrication processes," in *Advanced Fabrication Technologies for Micro/Nano Optics and Photonics*, vol. 6883 of *Proceedings of SPIE*, San Jose, Calif, USA, January 2008.

[33] E. di Fabrizio, F. Romanato, M. Gentill et al., "High-efficiency multilevel zone plates for keV X-rays," *Nature*, vol. 401, no. 6756, pp. 895–898, 1999.

[34] H. Dammann, "Blazed synthetic phase-only holograms," *Optik*, vol. 31, no. 1, pp. 95–104, 1970.

[35] M. Young, "Zone plates and their aberrations," *Journal of the Optical Society of America*, vol. 62, no. 8, pp. 972–976, 1972.

[36] M. Bautz, "Active pixel X-ray sensor technology development for the generation-X wide-field imager," in *White paper, Astro2010: The Astronomyand Astrophysics Decadal Survey*, EOS Discipline Program Panel, 2009.

[37] C. B. Wunderer, G. Weidenspointner, A. Zoglauer et al., "Germanium (compton) focal plane detectors for gamma-ray lenses," in *Space Telescopes and Instrumentation II: Ultraviolet to Gamma Ray*, vol. 6266 of *Proceedings of SPIE*, Orlando, Fla, USA, May 2006.

[38] Q. Li, A. Garson, P. Dowkontt et al., "Fabrication and test of pixelated CZT detectors with different pixel pitches and thicknesses," in *Proceedings of IEEE Nuclear Science Symposium (NSS '08)*, pp. 484–489, Dresden, Germany, October 2008.

[39] C. K. Stahle, D. McCammon, and K. D. Irwin, "Quantum calorimetry," *Physics Today*, vol. 52, no. 8, pp. 32–37, 1999.

[40] R. L. Kelley, S. R. Bandler, W. B. Doriese et al., "The X-ray microcalorimeter spectrometer for the international X-ray observatory," in *Proceedings of the 13th International Workshop on Low Temperature Detectors (LTD '09)*, B. Young, B. Cabrera, and A. Miller, Eds., vol. 1185 of *AIP Conference Series*, pp. 757–760, December 2009.

[41] B. X. Yang, "Fresnel and refractive lenses for X-rays," *Nuclear Instruments and Methods in Physics Research A*, vol. 328, no. 3, pp. 578–587, 1993.

[42] B. Nöhammer, C. David, J. Gobrecht, and H. P. Herzig, "Optimized staircase profiles for diffractive optical devices made from absorbing materials," *Optics Letters*, vol. 28, no. 13, pp. 1087–1089, 2003.

[43] N. White, "X-ray astronomy: imaging black holes," *Nature*, vol. 407, no. 6801, pp. 146–147, 2000.

[44] W. Cash, "Imaging a black hole: MAXIM," *Advances in Space Research*, vol. 35, no. 1, pp. 122–129, 2005.

[45] S. Gillessen, F. Eisenhauer, S. Trippe et al., "Monitoring stellar orbits around the massive black hole in the galactic center," *The Astrophysical Journal*, vol. 692, pp. 1075–1109, 2009.

[46] K. Gebhardt and J. Thomas, "The black hole mass, stellar mass-to-light ratio, and Dark Halo in m87," *Astrophysical Journal*, vol. 700, no. 2, pp. 1690–1701, 2009.

[47] E. Middelberg and U. Bach, "High resolution radio astronomy using very long baseline interferometry," *Reports on Progress in Physics*, vol. 71, no. 6, Article ID 066901, 2008.

[48] T. P. Krichbaum, D. A. Graham, M. Bremer et al., "Sub-milliarcsecond imaging of Sgr A* and M 87," *Journal of Physics: Conference Series*, vol. 54, no. 1, pp. 328–334, 2006.

[49] S. S. Doeleman, J. Weintroub, A. E. E. Rogers et al., "Event-horizon-scale structure in the supermassive black hole candidate at the Galactic Centre," *Nature*, vol. 455, no. 7209, pp. 78–80, 2008.

[50] Y. Murata, N. Mochizuki, H. Saito et al., "The next generation space VLBI project: VSOP-2," in *Proceedings of the International Astronomical Union*, J. M. Chapman and W. A. Baan, Eds., vol. 242 of *IAU Symposium*, pp. 517–521, 2007.

[51] P. J. Armitage and C. S. Reynolds, "The variability of accretion on to Schwarzschild black holes from turbulent magnetized discs," *Monthly Notices of the Royal Astronomical Society*, vol. 341, no. 3, pp. 1041–1050, 2003.

[52] T. P. Krichbaum, I. Agudo, U. Bach, A. Witzel, and J. A. Zensus, "VLBI at the highest frequencies—AGN studies with micro-arcsecond resolution," in *Proceedings of the 8th European VLBI Network Symposium*, 2006.

[53] J. Hevelius, "Machinae coelestis," vol. 2, p. 353, 1738.

[54] C. Braig and P. Predehl, "Efficient Fresnel x-ray optics made simple," *Applied Optics*, vol. 46, no. 14, pp. 2586–2599, 2007.

[55] C. Braig and P. Predehl, "A diffraction-limited dual-band X-ray telescope," in *Optics for EUV, X-Ray, and Gamma-Ray Astronomy III*, vol. 6688 of *Proceedings of SPIE*, San Diego, Calif, USA, August 2007.

[56] S. J. Bennett, "Achromatic combinations of hologram optical elements," *Applied Optics*, vol. 15, no. 2, pp. 542–545, 1976.

[57] D. A. Buralli and J. R. Rogers, "Some fundamental limitations of achromatic holographic systems," *Journal of the Optical Society of America A*, vol. 6, pp. 1863–1868, 1989.

[58] A. Michette, C. Buckley, F. Gallo, K. Powell, and S. Pfauntsch, "Zone plate achromatic doublets," in *Advances in X-Ray Optics*, A. K. Freund, T. Ishikawa, A. M. Khounsary, D. C. Mancini, A. G. Michette, and S. Oestreich, Eds., vol. 4145 of *Proceedings of SPIE*, pp. 303–310, San Diego, Calif, USA, August 2001.

[59] L. Koechlin, D. Serre, and P. Deba, "The Fresnel interferometric imager," *Astrophysics and Space Science*, vol. 320, no. 1–3, pp. 225–230, 2009.

[60] G. K. Skinner, "Design and imaging performance of achromatic diffractive-refractive x-ray and gamma-ray Fresnel lenses," *Applied Optics*, vol. 43, no. 25, pp. 4845–4853, 2004.

[61] P. Gorenstein, W. Cash, N. Gehrels et al., "The future of high angular resolution X-ray astronomy," in *Space Telescopes and Instrumentation 2008: Ultraviolet to Gamma Ray*, vol. 7011 of *Proceedings of SPIE*, Marseille, France, June 2008.

[62] T. Stone and N. George, "Hybrid diffractive-refractive lenses and achromats," *Applied Optics*, vol. 27, pp. 2960–2971, 1988.

[63] B. Lengeler, C. G. Schroer, M. Kuhlmann et al., "Refractive x-ray lenses," *Journal of Physics D*, vol. 38, no. 10, pp. A218–A222, 2005.

[64] C. Braig and P. Predehl, "Advanced Fresnel X-ray telescopes for spectroscopic imaging," *Experimental Astronomy*, vol. 27, no. 3, pp. 131–155, 2010.

[65] Y. Wang, W. Yun, and C. Jacobsen, "Achromatic fresnel optics for wideband extreme-ultraviolet and X-ray imaging," *Nature*, vol. 424, no. 6944, pp. 50–53, 2003.

[66] G. K. Skinner, "X-ray and gamma-ray focusing and interferometry," in *Optics for EUV, X-Ray, and Gamma-Ray Astronomy IV*, vol. 7437 of *Proceedings of SPIE*, San Diego, Calif, USA, August 2009.

[67] R. Smith, *A Compleat System of Optiks*, Gedani, 1673.

[68] M. J. Simpson and A. G. Michette, "Imaging properties of modified fresnel zone plates," *Optica Acta*, vol. 31, pp. 403–413, 1984.

[69] L. Kipp, M. Skibowski, R. L. Johnson et al., "Sharper images by focusing soft X-rays with photon sieves," *Nature*, vol. 414, no. 6860, pp. 184–188, 2001.

[70] F. Giménez, J. A. Monsoriu, W. D. Furlan, and A. Pons, "Fractal photon sieve," *Optics Express*, vol. 14, no. 25, pp. 11958–11963, 2006.

[71] G. Skinner, "Development of optics for sub-micro-arc-second angular resolution in the X-ray and gamma-ray domains," in *White paper, Astro2010: The Astronomy and Astrophysics Decadal Survey*, pp. 1–10, 2009.

[72] J. Sochacki, A. Klodziejczyk, Z. Jaroszewicz, and S. Bara, "Nonparaxial design of generalized axicons," *Applied Optics*, vol. 31, pp. 5326–5330, 1992.

[73] Q. Cao and S. Chi, "Axially symmetric on-axis flat-top beam," *Journal of the Optical Society of America A*, vol. 17, no. 3, pp. 447–455, 2000.

[74] P. Gorenstein, J. D. Phillips, and R. D. Reasenberg, "Refractive/diffractive telescope with very high angular resolution for X-ray astronomy," in *Optics for EUV, X-Ray, and Gamma-Ray Astronomy II*, O. Citterio and S. L. O'Dell, Eds., vol. 5900 of *Proceedings of SPIE*, pp. 1–8, San Diego, Calif, USA, August 2005.

[75] T. G. Farr, P. A. Rosen, E. Caro et al., "The shuttle radar topography mission," *Reviews of Geophysics*, vol. 45, no. 2, Article ID RG2004, 2007.

[76] A. N. Parmar, M. Arnaud, X. Barcons et al., "XEUS—the X-ray evolving universe spectroscopy mission," in *Space Telescopes and Instrumentation II: Ultraviolet to Gamma Ray*, vol. 6266 of *Proceedings of SPIE*, Orlando, Fla, USA, May 2006.

[77] J. Krizmanic, G. Skinner, and N. Gehrels, "Formation flying for a Fresnel lens observatory mission," *Experimental Astronomy*, vol. 20, no. 1–3, pp. 497–503, 2005.

[78] K. C. Gendreau, J. Leitner, L. Markley, W. C. Cash, and A. F. Shipley, "Requirements and options for a stable inertial reference frame for a 100-micro-arcsecond imaging telescope," in *Interferometry in Space*, M. Shao, Ed., vol. 4852 of *Proceedings of SPIE*, pp. 685–694, Waikoloa, Hawaii, USA, August 2002.

[79] R. J. Luquette and R. M. Sanner, "Spacecraft formation control: Managing line-of-sight drift based on the dynamics of relative motion," in *Proceedings of the 3rd International Symposium on Formation Flying, Missions and Technologies (ESA-ESTEC '08)*, Noordwijk, The Netherlands, April 2008.

[80] N. Meidinger, R. Andritschke, S. Ebermayer et al., "CCD detectors for spectroscopy and imaging of x-rays with the

eROSITA space telescope," in *UV, X-Ray, and Gamma-Ray Space Instrumentation for Astronomy XVI*, vol. 7435 of *Proceeding of SPIE*, San Diego, Calif, USA, August 2009.

[81] J. Treis, R. Andritschke, R. Hartmann et al., "Pixel detectors for x-ray imaging spectroscopy in space," *Journal of Instrumentation*, vol. 4, no. 3, Article ID P03012, 2009.

[82] A. Laborie, R. Davancens, P. Pouny et al., "The Gaia focal plane," in *Focal Plane Arrays for Space Telescopes III*, vol. 6690 of *Proceedings of SPIE*, San Diego, Calif, USA, August 2007.

[83] R. Hyde, S. Dixit, A. Weisberg, and M. Rushford, "Eyeglass: a very large aperture diffractive space telescope," in *Highly Innovative Space Telescope Concepts*, H. A. MacEwen, Ed., vol. 4849 of *Proceedings of SPIE*, pp. 28–39, Waikoloa, Hawaii, USA, 2002.

[84] R. Hyde and S. Dixit, "A giant leap for space telescopes," LNL Science and Technology Review, https://www.llnl.gov/str/March03/Hyde.html.

[85] G. K. Skinner and J. F. Krizmanic, "X-ray interferometry with transmissive beam combiners for ultra-high angular resolution astronomy," *Experimental Astronomy*, vol. 27, no. 1-2, pp. 61–76, 2009.

[86] W. Cash, "Maxim: micro-arcsecond x-ray imaging mission," in *Interferometry in Space*, M. Shao, Ed., vol. 4852 of *Proceedings of SPIE*, pp. 196–209, Waikoloa, Hawaii, USA, August 2003.

[87] J. Krizmanic, B. Morgan, R. Streitmatter et al., "Development of ground-testable phase fresnel lenses in silicon," *Experimental Astronomy*, vol. 20, no. 1–3, pp. 299–306, 2005.

[88] B. Morgan, C. M. Waits, J. Krizmanic, and R. Ghodssi, "Development of a deep silicon phase fresnel lens using gray-scale lithography and deep reactive ion etching," *Journal of Microelectromechanical Systems*, vol. 13, no. 1, pp. 113–120, 2004.

[89] Z. Arzoumanian, K. C. Gendreau, W. C. Cash, A. F. Shipley, and S. Z. Queen, "Laboratory testbeds for broadband X-ray interferometry," in *UV and Gamma-Ray Space Telescope Systems*, G. Hasinger and M. J. L. Turner, Eds., vol. 5488 of *Proceedings of SPIE*, pp. 623–629, Glasgow, UK, June 2004.

[90] G. Gendreau, "GSFC X-ray Interferometry Testbed," http://xraybeamline.gsfc.nasa.gov/.

[91] J. Krizmanic, In preparation.

[92] G. K. Skinner, Z. Arzoumanian, W. C. Cash et al., "The milli-arc-second structure imager (MASSIM): a new concept for a high angular resolution x-ray telescope," in *Space Telescopes and Instrumentation 2008: Ultraviolet to Gamma Ray*, vol. 7011 of *Proceedings of SPIE*, Marseille, France, June 2008.